Inorganic Chemistry

pubs.acs.org/IC

Communication

Application of High-Energy-Resolution X-ray Absorption Spectroscopy at the U L_3-Edge to Assess the U(V) Electronic Structure in $FeUO_4$

Takumi Yomogida,* Daisuke Akiyama, Kazuki Ouchi, Yuta Kumagai, Kotaro Higashi, Yoshihiro Kitatsuji, Akira Kirishima, Naomi Kawamura, and Yoshio Takahashi

Cite This: *Inorg. Chem.* 2022, 61, 20206−20210

Read Online

ACCESS | Metrics & More | Article Recommendations | Supporting Information

ABSTRACT: $FeUO_4$ was studied to clarify the electronic structure of U(V) in a metal monouranate compound. We obtained the peak splitting of spectra utilizing high-energy-resolution fluorescence detection−X-ray absorption near-edge structure (HERFD-XANES) spectroscopy at the U L_3-edge, which is a novel technique in uranium(V) monouranate compounds. Theoretical calculations revealed that the peak splitting was caused by splitting of the 6d orbital of U(V) in $FeUO_4$, which would be used to detect minor U(V) species. Such distinctive electronic states are of major interest to researchers and engineers working in various fields, from fundamental physics to the nuclear industry and environmental sciences for actinide elements.

Uranium (U), used as a fuel for nuclear power generation, is an important element in actinide chemistry, nuclear technology, and environmental science due to its usefulness as an energy resource and chemical toxicity.[1] The oxidation state of U is a critical factor in understanding its migration behavior in the environment. It is predominantly present in the environment as U(IV) and U(VI) species. U(V), a minor chemical species of U, is less common. However, recent studies have reported that U(V) is relatively stable in magnetite,[2−5] goethite,[6] and depleted U.[7] Its unique characteristics were reported as intermediates during the reduction of U(VI) to U(IV).[2,6,8−11] Therefore, U(V) compounds have attracted attention in geological, environmental, and actinide chemistry studies.

$FeUO_4$ (Figure 1) is a metal monouranate compound containing U(V). It was first studied by Bacmann et al. in 1967.[12] It has a $BiVO_4$-like structure in space group *Pbcn* with lattice constants a = 4.88 Å, b = 11.93 Å, and c = 5.11 Å.[13] The U and iron (Fe) coordination environments in $FeUO_4$ consist of distorted octahedra, $[UO_6]$ and $[FeO_6]$, with two short axial U−O (2.0465 Å) and Fe−O (1.9913 Å) bonds and four long equatorial U−O (2.1820 and 2.2154 Å) and Fe−O (2.0515 and 2.0901 Å) bonds. Recently, Crean et al. found that $FeUO_4$ was produced in association with depleted U in the environment.[7] The occurrence of $FeUO_4$ demonstrates the stability of this phase for more than 25 years in the surface environment. Furthermore, Akiyama et al. reported that $FeUO_4$ could be generated under the Fukushima Dai-ichi Nuclear Power Station's severe accident conditions.[14] Few studies exist on the electronic structure of $FeUO_4$.[7,14−16] Guo et al. reported that all U ions in $FeUO_4$ would be a 5+ oxidation state by DFT+U calculations (DFT = density functional theory), whereas the U^{5+}/U ratio in $FeUO_4$ is 66.4%, as determined by X-ray photoelectron spectroscopy analysis in the U 4f region.[15] Because of the possibility of surface oxidation, the U^{5+}/U ratio does not represent the U valence information for the bulk samples. Detailed analysis is indispensable to discuss the electronic structure of U in the $FeUO_4$ compound.

X-ray absorption near-edge structure spectroscopy (XANES) has been widely used for characterizing the electronic structure of U materials.[15−18] This is due to its several advantages, including element-selective measurement, easy sample preparation, and nondestructive analysis. U L- and M-edge XANES spectroscopy has been used to analyze U compounds. The energy range of the U M-edge lies in soft X-ray region (3.5−3.7 keV), which makes the XANES measurement difficult due to X-ray absorption by air compared to U L_3-edge XANES measurements. The U has a L_3-edge (17.2 keV) in the hard-X-ray region, and consequently the radioactive samples can be sealed by films for safety of the experiments. Because of these advantages, several U(V) compounds[17] and $FeUO_4$[15,16] have been analyzed so far by U L_3-edge XANES spectroscopy. Soldatov et al. showed that there is a small preedge shoulder in the absorption spectra of $NaUO_3$, KUO_3, and $RbUO_3$.[17] They also reported the XANES spectra of KUO_3 and $RbUO_3$ in a perfect perovskite structure with two more notable postedge shoulders. Misa et al. reported the XANES spectrum of $Tl_2U_4O_{12}$, another uranium(V) uranate in a defective pyrochlore structure with significant shifts in the energy positions of the white line and postedge shoulder.[18] The occurrence and positions of pre- and postedge

Received: September 9, 2022
Published: December 2, 2022

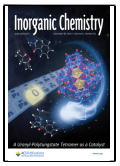

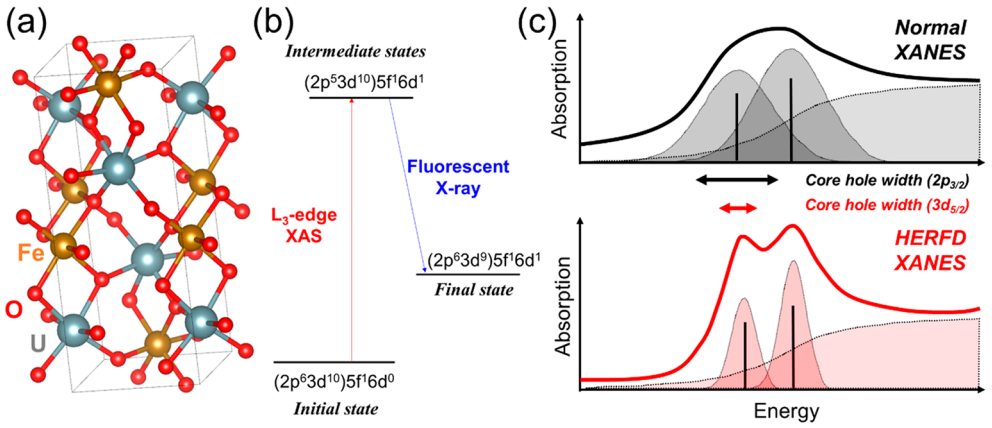

Figure 1. (a) Representation of the $FeUO_4$ unit cell, exhibiting an ideal structure. The oxygen atoms form a framework of oxygen octahedra around each U atom and Fe atom. This figure was created using *VESTA3* software. (b) Simplified and schematic overview of the U theoretical valence configuration evolution during XANES (normal XANES and HERFD-XANES) for U^{5+} valence states at the U L_3-edges. Note that only the shells involved in the measured transitions are reported. The core−shells are in brackets to distinguish them from the valence shells. (c) Schematic overview of the difference of normal XANES and HERFD-XANES spectra.

shoulders depends on the structure of the U(V) compounds. A detailed study on the differences between these peaks is expected to be useful in discriminating compounds containing U(V). Some researchers reported the U L_3-edge XANES spectrum of $FeUO_4$, a small preedge shoulder.[15,16] However, the origin of the characteristic microstructures of the U L_3-edge XANES spectrum of $FeUO_4$ was not discussed in the previous literature.

Recently, high-energy-resolution fluorescence detection (HERFD)-XANES has been applied to various U compounds as a more sensitive method for analyzing the electronic structures.[19−27] The energy resolution of a normal XANES spectrum depends on the core−hole lifetime broadening in the final state. In a standard transmission mode of the U L_3-edge XANES experiment, the $2p_{3/2}$ core−hole lifetime broadening is 7.8 eV for U.[28] In a fluorescence mode of the U L_3-edge XANES experiment, the XANES spectrum is obtained by monitoring the $L\alpha_1$ emission line (Figure 1b). The overall spectral energy resolution is limited by the energy resolution of the solid-state detector (SSD) because the energy resolution of the SSD is 100 eV or even worse. The spectral feature of XANES is limited by the lifetime of the $3d_{5/2}$ core−hole in the final transition state, which is affected by the large lifetime broadening of the $2p_{3/2}$ core−hole (Figure 1c). On the other hand, using an X-ray emission spectrometer, a high-energy resolution of a few electronvolts can be achieved, which enables measurement of the spectral width below the inner-shell core−hole lifetime width. In this case, the spectral feature of XANES is limited not by the lifetime of the $2p_{3/2}$ core−hole but by the lifetime of the sharper $3d_{5/2}$ states (4 eV) of the final state[29] (Figure 1c). Kvashnina et al. reported a change in the peak shape of UO_2 by performing U L_3-edge HERFD-XANES measurements.[22] The peak shape showed that crystal-field splitting of the U 6d states between e_g and t_{2g} orbitals. Bao et al. reported peak splitting of the $Th_{1-x}U_xO_2$ compounds in the thorium (Th) L_3-edge HERFD-XANES spectra and observed the crystal-field splitting (~3.5 eV) between the 6d e_g and t_{2g} orbitals in $Th_{1-x}U_xO_2$ compounds.[30] Therefore, the HERFD-XANES spectra exhibit distinctive microstructures that were invisible in the normal XANES.

As an example of HERFD-XANES analysis of uranium(V) monouranate compounds, KUO_3 has recently been reported.[25,27] Finite-difference methods for near-edge structure (FDMNES)[31] simulations showed that the peak-splitting width of the U(V) compound is about 7 eV,[27] indicating that the characteristic peak splitting of U(V) in $FeUO_4$ could be observed by measuring with an energy resolution sufficiently higher than the width of the $3d_{5/2}$ core−hole lifetime.

In this paper, our group presents the results on the measured HERFD-XANES spectra of $FeUO_4$ for the first time. To our knowledge, this is the first report of such measurements in published literature. Furthermore, we have achieved a high energy resolution of ca. 1.7 eV by using incident X-ray with a high energy resolution (1.2 eV) and by precisely focusing X-ray fluorescence (XRF) with an X-ray emission spectrometer.[26,32] By measuring with the high energy resolution, we succeeded in detecting a specific peak splitting of U(V) in $FeUO_4$, which could not be detected in normal XANES spectra. We here discuss whether theoretical calculations by FDMNES correlate this peak splitting with the 6d orbital at the transition state by comparing it with UO_2 and $UO_2(NO_3)_2(H_2O)_6$, for which HERFD-XANES analysis and FDMNES simulations have already been reported.[19]

The $FeUO_4$ sample that we used in HERFD-XANES measurements was already characterized in previous literature.[14,16] X-ray diffraction profile of the $FeUO_4$ sample is shown in Figure S1. Fe species in $FeUO_4$ were evaluated to be trivalent by Fe K-edge XANES spectroscopy and ^{57}Fe Mössbauer spectroscopy. The HERFD-XANES experiments were performed at beamline BL39XU, SPring-8, as previously reported.[26] A combined (incident convoluted with emitted) energy resolution of ~1.7 eV was achieved in the experiments, as determined by measuring the full width at half-maximum (fwhm). The detailed conditions of the experiment are described in the Supporting Information (SI). The HERFD-XANES spectrum at the U L_3-edge of UO_2, $FeUO_4$, and $UO_2(NO_3)_2(H_2O)_6$ collected by monitoring the $L\alpha_1$ emission line and the corresponding XANES spectrum collected in the conventional fluorescence mode are compared in Figure 2. The white line at approximately 17178 eV in the conventional XANES spectrum of $FeUO_4$ mainly originates from the electronic transition from U $2p_{3/2}$ to unoccupied 6d states. Soldatov et al. reported that a lower-energy shoulder observed in the U L_3-edge XANES spectrum is an intrinsic feature of the

https://doi.org/10.1021/acs.inorgchem.2c03208
Inorg. Chem. 2022, 61, 20206−20210

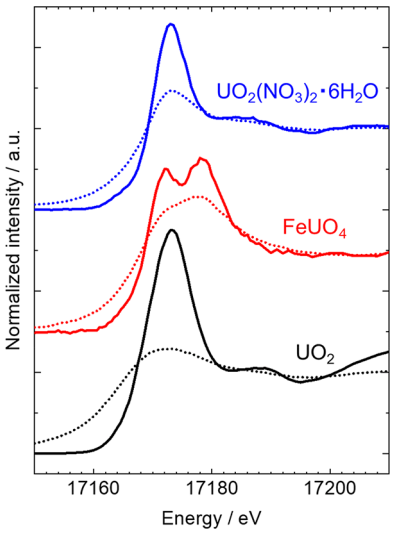

Figure 2. (Solid line) U L_3-edge HERFD-XANES spectra of UO_2 (black), $FeUO_4$ (red), and $UO_2(NO_3)_2 \cdot 6H_2O$ (blue) recorded using the X-ray emission spectrometer set to the Lα_1 emission energy. (Dotted line) Conventional XANES spectra of UO_2 (black), $FeUO_4$ (red), and $UO_2(NO_3)_2 \cdot 6H_2O$ (blue) collected in fluorescence mode by a SSD.

unoccupied U 6d electronic states of the U(V) compound by measuring the normal XANES spectra of $NaUO_3$, KUO_3, and $RbUO_3$.[17] The XANES spectrum of $FeUO_4$ was characterized by a shoulder around 17172 eV and a peak top around 17180 eV. The features of the XANES structure of $FeUO_4$ were consistent with previous publications in the literature.[15,16] The HERFD-XANES spectrum of the same sample, the red line in Figure 2, showed more remarkable features: the white line was split into two peaks in the HERFD-XANES spectra. The conventional and HERFD-XANES spectra of UO_2 and $UO_2(NO_3)_2(H_2O)_6$ measured at the same energy resolution are also shown in Figure 2; no peak splitting was observed in the case of UO_2 and $UO_2(NO_3)_2(H_2O)_6$.

The experimental $FeUO_4$ HERFD-XANES spectra were compared to that calculated by FDMNES in Figure 3. In a previous study, the preedge feature of the HERFD-XANES spectra was attributed to the quadrupole component of the

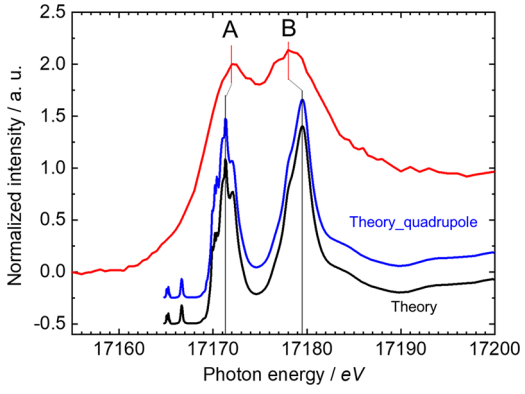

Figure 3. U L_3-edge HERFD-XANES spectrum (red line) of $FeUO_4$ and comparisons with the theoretical calculations (FDMNES) with (blue line, Theory_quadrupole) and without (black line, Theory) $2p_{3/2} \rightarrow 5f$ electronic transitions. The first peak is labeled A, and the second peak is labeled B.

electronic transitions from $2p_{3/2}$ to the partially empty U f shells.[19,33] Calculations were performed with and without consideration of the $2p_{3/2} \rightarrow 5f$ transitions, and no experimental broadening was included. The theoretical calculation showed a split into two energy levels, reflecting the splitting of the 6d band. The simulated split width of the theoretical calculation was about 8 eV, which is almost consistent with the experimental peak splitting width of about 6 eV (Table 1). Furthermore, all theoretical spectra of $FeUO_4$

Table 1. Energy Positions (eV) of the Experimentally Observed and Calculated U L_3-Edge HERFD-XANES Edge and Postedge Spectral Features

	$FeUO_4$ (this study)		KUO_3 (ref27)	
feature	experimental	calculated	experimental	calculated
A	17172(1)	17171.3(2)	17173(1)	17173.3(2)
B	17178(1)	17179.5(2)	17179.6(5)	17180.2(2)
energy separation	6(2)	8.2(4)	6.6(1.5)	6.9(4)

reproduced the general shape and number of postedge resonances in the HERFD-XANES spectra, as shown in Figure S2. The postedge structure labeled in C (17228 eV; Figure S2) was also reproduced by the calculation (17225 eV). Despite the minor difference between the FDMNES calculations and experimental HERFD-XANES possibly due to the muffin-tin approximation in the simulation, the theoretical calculation reproduces the experimental spectra reasonably well. These differences could be improved by more precise electronic structure calculations. Therefore, the peak splitting of the $FeUO_4$ HERFD-XANES spectrum was observed from both experiments and simulations.

On the other hand, when the UO_2 sample was measured with the same energy resolution, no peak splitting was observed, as mentioned earlier (Figure 2). As shown in Figure S3, the simulation assumes a splitting of the 6d band (ca. 4 eV) of UO_2. Kvashnina et al. reported a change in the peak shape of UO_2 by performing HERFD-XANES measurements using XRF of the Lβ_5 line. The broadening of the spectral features in the Lβ_5 line is related to core−hole lifetime broadenings for the U 5d and 2p levels,[34] which showed a smaller core−hole lifetime broadening effect compared to using the Lα_1 line ($3d_{5/2}$ states) for HERFD-XANES measurements.[22,24] However, use of the Lα_1 line is better to increase the sensitivity of the method, which should be important in applying the method to more dilute samples such as environmental samples, which is our target in the future. They also reported that no change in the peak shape was observed when the Lα_1 line was used,[22] as found in our study. Compared to the FDMNES simulation results for $FeUO_4$ (Figure 3) and UO_2 (Figure S3), the peak height of the first (~17171 eV) and second (~17180 eV) intense peaks had almost the same heights and widths in the simulation of $FeUO_4$. In contrast, the peak around 17172 eV was of low intensity, and the peak width was thinner than that of the peak around 17176 eV in the simulation of UO_2 (Figure S3). Furthermore, Figure S3 shows that the width of the peak splitting was also small, about 4 eV. For these reasons, the peak splitting of UO_2 could not be observed. Therefore, the intensity and width of the band of $FeUO_4$ would be a factor in observing the peak splitting.

In the HERFD-XANES spectra of U compounds, the participation of 5f orbitals in U−O bonding has been discussed

https://doi.org/10.1021/acs.inorgchem.2c03208
Inorg. Chem. 2022, 61, 20206−20210

by several authors.[19,22,33] To estimate the participation of 5f orbitals in the peak splitting, we compared the U unoccupied angular momentum projected density of states (d/f-DOS). Figure S4 shows that the mixing of U d and U f empty valence states on the absorption edge was observed around 17170 eV. However, no distinct preedge peak around 17165 eV from the quadrupolar $2p_{3/2} \rightarrow 5f$ electronic transition was observed compared to measurements of the $[UO_2Py_5][KI_2Py_2]$ and $UO_2(NO_3)_26H_2O$ compounds, which have been reported in a previous study.[19] The peak splitting in the HERFD-XANES spectrum of $FeUO_4$ is not significantly affected by $2p_{3/2} \rightarrow 5f$ electronic transitions and is due to splitting of the 6d orbital, as in the case of KUO_3.[27]

The results indicate that the peak splitting of the HERFD-XANES spectrum of $FeUO_4$ originates from the 6d orbital. The HERFD-XANES spectrum of KUO_3 was measured as a compound of U(V) in previous reports.[25,27] Table 1 shows the observed HERFD-XANES peak positions in $FeUO_4$ and KUO_3. The calculated peak-splitting width was 8.2 eV for $FeUO_4$, which is larger than the 6.9 eV value for KUO_3.[27] The result showed that the crystal-field splitting of $FeUO_4$ is larger than that of KUO_3, which is one of the reasons that the peak splitting was clearly observed in $FeUO_4$. In the FDMNES simulations of KUO_3, a peak splitting at about 7 eV was observed because of strong crystal-field splitting, but the peak splitting was not fully deconvoluted in the experimental spectra in the previous studies. They performed the HERFD-XANES measurement with an energy resolution of 3.7 eV, which is the closest value to the lifetime width of $3d_{5/2}$, resulting in a larger broadening of the peak shape. However, in our study, the peak splitting of the HERFD-XANES spectrum of $FeUO_4$ was almost the same as the theoretical calculation that was observed by measuring HERFD-XANES with extremely high energy resolution (<1.7 eV). These results indicated that the high energy resolution at the HERFD-XANES measurements was indispensable for detecting the characteristic peak splitting of U(V) in $FeUO_4$.

In conclusion, we obtained the HERFD-XANES spectrum of $FeUO_4$, a U(V)-containing compound. Using a high-energy-resolution (ca. 1.7 eV) X-ray emission spectrometer, we observed a peak splitting of the HERFD-XANES spectrum of $FeUO_4$ that has not been observed in conventional XANES. The results indicated that HERFD-XANES measurements of U(V) in $FeUO_4$ with high energy resolution provide spectra with remarkable microstructure. Theoretical calculations with the FDMNES code indicated that the peak splitting was due to the $2p_{3/2} \rightarrow 6d$ electronic transition. Theoretical calculations reproduced the peak splitting well, indicating that HERFD-XANES was useful for a detailed understanding of the electronic structure of U(V) compounds. This peak splitting could be observed in other U(V) compounds, and we are currently analyzing other U(V) compounds and planning to clarify the origin of the peak splitting by discussing the differences in the crystal structure.

■ ASSOCIATED CONTENT

Supporting Information

The Supporting Information is available free of charge at https://pubs.acs.org/doi/10.1021/acs.inorgchem.2c03208.

Experimental and calculation methods, sample preparation, XANES and HERFD-XANES measurements, and FDMNES calculations (PDF)

■ AUTHOR INFORMATION

Corresponding Author

Takumi Yomogida − *Department of Earth and Planetary Science, The University of Tokyo, Bunkyo, Tokyo 113-0033, Japan; Nuclear Science and Engineering Center, Japan Atomic Energy Agency, Tokai-mura, Naka-gun, Ibaraki 319-1195, Japan;* orcid.org/0000-0002-2005-0027; Email: yomogida.takumi@jaea.go.jp

Authors

Daisuke Akiyama − *Institute of Multidisciplinary Research for Advanced Materials, Tohoku University, Aoba, Sendai, Miyagi 980-8577, Japan*

Kazuki Ouchi − *Nuclear Science and Engineering Center, Japan Atomic Energy Agency, Tokai-mura, Naka-gun, Ibaraki 319-1195, Japan*

Yuta Kumagai − *Nuclear Science and Engineering Center, Japan Atomic Energy Agency, Tokai-mura, Naka-gun, Ibaraki 319-1195, Japan;* orcid.org/0000-0002-9149-0185

Kotaro Higashi − *Center for Synchrotron Radiation Research, Japan Synchrotron Radiation Research Institute (JASRI), Sayo, Hyogo 679-5198, Japan*

Yoshihiro Kitatsuji − *Nuclear Science and Engineering Center, Japan Atomic Energy Agency, Tokai-mura, Naka-gun, Ibaraki 319-1195, Japan*

Akira Kirishima − *Institute of Multidisciplinary Research for Advanced Materials, Tohoku University, Aoba, Sendai, Miyagi 980-8577, Japan*

Naomi Kawamura − *Center for Synchrotron Radiation Research, Japan Synchrotron Radiation Research Institute (JASRI), Sayo, Hyogo 679-5198, Japan*

Yoshio Takahashi − *Department of Earth and Planetary Science, The University of Tokyo, Bunkyo, Tokyo 113-0033, Japan; Isotope Science Center, University of Tokyo, Bunkyo, Tokyo 113-0032, Japan; Photon Factory, Institute of Materials Structure Science, High Energy Accelerator Research Organization, KEK, Tsukuba, Ibaraki 305-0801, Japan*

Complete contact information is available at: https://pubs.acs.org/10.1021/acs.inorgchem.2c03208

Author Contributions

T.Y. and Y.T. designed the research and wrote the paper. T.Y. performed the sample preparation, HERFD-XANES measurements and analyses, and FDMNES simulation. D.A. performed the sample preparation for $FeUO_4$ and UO_2. K.O. and Y.K. performed the sample preparation for XANES measurements. A.K. and Y.K. provided helpful suggestions for the research. K.H. and N.K. supported the HERFD-XANES measurements using a X-ray emission spectrometer. All of the authors discussed the results and contributed to the manuscript.

Notes

The authors declare no competing financial interest.

■ ACKNOWLEDGMENTS

This work was supported by a JSPS KAKENHI Grant-in-Aid for Early-Career Scientists (Grant 19K15606). This study was performed with the approval of JASRI/SPring-8 (Proposal Nos. 2020A0174, 2020A1566, 2021B1821, and 2022A1733).

REFERENCES

(1) Romanchuk, A. Y.; Vlasova, I. E.; Kalmykov, S. N. Speciation of Uranium and Plutonium From Nuclear Legacy Sites to the Environment: A Mini Review. *Front. Chem.* **2020**, *8*. DOI: 10.3389/fchem.2020.00630.

(2) Roberts, H. E.; Morris, K.; Law, G. T. W.; Mosselmans, J. F. W.; Bots, P.; Kvashnina, K.; Shaw, S. Uranium(V) Incorporation Mechanisms and Stability in Fe(II)/Fe(III) (oxyhydr)Oxides. *Environ.Sci. Technol. Lett.* **2017**, *4* (10), 421−426.

(3) Pidchenko, I.; Kvashnina, K. O.; Yokosawa, T.; Finck, N.; Bahl, S.; Schild, D.; Polly, R.; Bohnert, E.; Rossberg, A.; Gottlicher, J.; Dardenne, K.; Rothe, J.; Schafer, T.; Geckeis, H.; Vitova, T. Uranium Redox Transformations after U(VI) Coprecipitation with Magnetite Nanoparticles. *Environ. Sci. Technol.* **2017**, *51* (4), 2217−2225.

(4) Pan, Z.; Roebbert, Y.; Beck, A.; Bartova, B.; Vitova, T.; Weyer, S.; Bernier-Latmani, R. Persistence of the Isotopic Signature of Pentavalent Uranium in Magnetite. *Environ. Sci. Technol.* **2022**, *56* (3), 1753−1762.

(5) Yuan, K.; Antonio, M. R.; Ilton, E. S.; Li, Z.; Becker, U. Pentavalent Uranium Enriched Mineral Surface under Electrochemically Controlled Reducing Environments. *ACS Earth and Space Chem.* **2022**, *6* (5), 1204−1212.

(6) Stagg, O.; Morris, K.; Lam, A.; Navrotsky, A.; Velazquez, J. M.; Schacherl, B.; Vitova, T.; Rothe, J.; Galanzew, J.; Neumann, A.; Lythgoe, P.; Abrahamsen-Mills, L.; Shaw, S. Fe(II) Induced Reduction of Incorporated U(VI) to U(V) in Goethite. *Environ. Sci. Technol.* **2021**, *55* (24), 16445−16454.

(7) Crean, D. E.; Stennett, M. C.; Livens, F. R.; Grolimund, D.; Borca, C. N.; Hyatt, N. C. Multimodal X-ray microanalysis of a $UFeO_4$: evidence for the environmental stability of ternary U(v) oxides from depleted uranium munitions testing. *Environ. Sci. Process Impacts* **2020**, *22* (7), 1577−1585.

(8) Kushwaha, S.; Sreedhar, B.; Padmaja, P. XPS, EXAFS, and FTIR As Tools To Probe the Unexpected Adsorption-Coupled Reduction of U(VI) to U(V) and U(IV) on Borassus flabellifer-Based Adsorbents. *Langmuir* **2012**, *28* (46), 16038−16048.

(9) Yuan, K.; Ilton, E. S.; Antonio, M. R.; Li, Z.; Cook, P. J.; Becker, U. Electrochemical and Spectroscopic Evidence on the One-Electron Reduction of U(VI) to U(V) on Magnetite. *Environ. Sci. Technol.* **2015**, *49* (10), 6206−6213.

(10) Dewey, C.; Sokaras, D.; Kroll, T.; Bargar, J. R.; Fendorf, S. Calcium-Uranyl-Carbonato Species Kinetically Limit U(VI) Reduction by Fe(II) and Lead to U(V)-Bearing Ferrihydrite. *Environ. Sci. Technol.* **2020**, *54* (10), 6021−6030.

(11) Pan, Z.; Bártová, B.; LaGrange, T.; Butorin, S. M.; Hyatt, N. C.; Stennett, M. C.; Kvashnina, K. O.; Bernier-Latmani, R. Nanoscale mechanism of UO_2 formation through uranium reduction by magnetite. *Nat. Commun.* **2020**, *11*, 4001.

(12) Bacmann, M.; Bertaut, E. F. Structure du Mouveau Compose $UFeO_4$. *Bull. Soc. Fr. Mineral. Cristallogr.* **1967**, *90* (2), 257.

(13) Bacmann, M.; Bertaut, E. F.; Blaise, A.; Chevalier, R.; Roult, G. Magnetic Structures and Properties of $UFeO_4$. *J. Appl. Phys.* **1969**, *40* (3), 1131−1132.

(14) Akiyama, D.; Kusaka, R.; Kumagai, Y.; Nakada, M.; Watanabe, M.; Okamoto, Y.; Nagai, T.; Sato, N.; Kirishima, A. Study on the relation between the crystal structure and thermal stability of $FeUO_4$ and $CrUO_4$. *J. Nucl. Mater.* **2022**, *568*, 153847.

(15) Guo, X.; Tiferet, E.; Qi, L.; Solomon, J. M.; Lanzirotti, A.; Newville, M.; Engelhard, M. H.; Kukkadapu, R. K.; Wu, D.; Ilton, E. S.; Asta, M.; Sutton, S. R.; Xu, H.; Navrotsky, A. U(V) in metal uranates: a combined experimental and theoretical study of $MgUO_4$, $CrUO_4$, and $FeUO_4$. *Dalton Trans.* **2016**, *45* (11), 4622−4632.

(16) Akiyama, D.; Akiyama, H.; Uehara, A.; Kirishima, A.; Sato, N. Phase analysis of uranium oxides after reaction with stainless steel components and ZrO_2 at high temperature by XRD, XAFS, and SEM/EDX. *J. Nucl. Mater.* **2019**, *520*, 27−33.

(17) Soldatov, A. V.; Lamoen, D.; Konstantinović, M. J.; Van den Berghe, S.; Scheinost, A. C.; Verwerft, M. Local structure and oxidation state of uranium in some ternary oxides: X-ray absorption analysis. *J. Solid. State. Chem.* **2007**, *180* (1), 54−61.

(18) Misra, N. L.; Lahiri, D.; Singh Mudher, K. D.; Olivi, L.; Sharma, S. M. XANES study on novel mixed valent $A_2U_4O_{12}$(A = K, Rb or Tl) uranates. *X-Ray Spectrom.* **2008**, *37* (3), 215−218.

(19) Vitova, T.; Kvashnina, K. O.; Nocton, G.; Sukharina, G.; Denecke, M. A.; Butorin, S. M.; Mazzanti, M.; Caciuffo, R.; Soldatov, A.; Behrends, T.; Geckeis, H. High energy resolution x-ray absorption spectroscopy study of uranium in varying valence states. *Phys. Rev. B* **2010**, *82* (23). DOI: 10.1103/PhysRevB.82.235118.

(20) Glatzel, P.; Weng, T.-C.; Kvashnina, K.; Swarbrick, J.; Sikora, M.; Gallo, E.; Smolentsev, N.; Mori, R. A. Reflections on hard X-ray photon-in/photon-out spectroscopy for electronic structure studies. *J. Electron Spectrosc. Relat. Phenom.* **2013**, *188*, 17−25.

(21) Kvashnina, K. O.; de Groot, F. M. F. Invisible structures in the X-ray absorption spectra of actinides. *J. Electron Spectrosc. Relat. Phenom.* **2014**, *194*, 88−93.

(22) Kvashnina, K. O.; Kvashnin, Y. O.; Butorin, S. M. Role of resonant inelastic X-ray scattering in high-resolution core-level spectroscopy of actinide materials. *J. Electron Spectrosc. Relat. Phenom.* **2014**, *194*, 27−36.

(23) Walshe, A.; Prussmann, T.; Vitova, T.; Baker, R. J. An EXAFS and HR-XANES study of the uranyl peroxides $[UO_2(\eta_2\text{-}O_2)(H_2O)_2]\cdot nH_2O$ (n = 0, 2) and uranyl (oxy)hydroxide $[(UO_2)_4O(OH)_6]\cdot 6H_2O$. *Dalton Trans.* **2014**, *43* (11), 4400−4407.

(24) Kvashnina, K. O.; Kvashnin, Y. O.; Vegelius, J. R.; Bosak, A.; Martin, P. M.; Butorin, S. M. Sensitivity to actinide doping of uranium compounds by resonant inelastic X-ray scattering at uranium L_3 edge. *Anal. Chem.* **2015**, *87* (17), 8772−8780.

(25) Leinders, G.; Bes, R.; Kvashnina, K. O.; Verwerft, M. Local Structure in U(IV) and U(V) Environments: The Case of U_3O_7. *Inorg. Chem.* **2020**, *59* (7), 4576−4587.

(26) Kawamura, N.; Hrose, Y.; Honda, F.; Shimokasa, R.; Ishimatsu, N.; Mizumaki, M.; Kawaguchi, S. I.; Hirao, N.; Mimura, K. Study on the Correlation of U Valence States with U−U Distance in UPd_2Cd_{20}. *International Conference on Strongly Correlated Electron Systems (SCES2019)*, Okayama, Japan, Sept 23−28, 2019; SCES, 2020; Vol. *30*, p 011172. DOI: 10.7566/JPSCP.30.011172.

(27) Bes, R.; Leinders, G.; Kvashnina, K. Application of multi-edge HERFD-XAS to assess the uranium valence electronic structure in potassium uranate (KUO_3). *J. Synchrotron Radiat.* **2022**, *29* (1), 21.

(28) Krause, M. O.; Oliver, J. H. Natural widths of atomic K and L levels, Kα X-ray lines and several KLL Auger lines. *J. Phys. Chem. Ref. Data* **1979**, *8* (2), 329−338.

(29) Keski-Rahkonen, O.; Krause, M. O. Uranium *M* x-ray emission spectrum. *Phys. Rev. A* **1977**, *15* (3), 959−966.

(30) Bao, H.; Duan, P.; Zhou, J.; Cao, H.; Li, J.; Yu, H.; Jiang, Z.; Liu, H.; Zhang, L.; Lin, J.; Chen, N.; Lin, X.; Liu, Y.; Huang, Y.; Wang, J.-Q. Uranium-Induced Changes in Crystal-Field and Covalency Effects of Th^{4+} in $Th_{1-x}U_xO_2$ Mixed Oxides Probed by High-Resolution X-ray Absorption Spectroscopy. *Inorg. Chem.* **2018**, *57* (18), 11404−11413.

(31) Joly, Y. X-ray absorption near-edge structure calculations beyond the muffin-tin approximation. *Phys. Rev. B* **2001**, *63* (12). DOI: 10.1103/PhysRevB.63.125120.

(32) Asakura, H.; Tanaka, T. Recent Applications of X-ray Absorption Spectroscopy in Combination with High Energy Resolution Fluorescence Detection. *Chem. Lett.* **2021**, *50* (5), 1075−1085.

(33) Bes, R.; Rivenet, M.; Solari, P. L.; Kvashnina, K. O.; Scheinost, A. C.; Martin, P. M. Use of HERFD-XANES at the U L_3- and M_4-Edges To Determine the Uranium Valence State on $[Ni(H_2O)_4]_3[U(OH,H_2O)(UO_2)_8O_{12}(OH)_3]$. *Inorg. Chem.* **2016**, *55* (9), 4260−4270.

(34) de Groot, F. M. F.; Krisch, M. H.; Vogel, J. Spectral sharpening of the Pt L edges by high-resolution x-ray emission. *Phys. Rev. B* **2002**, *66* (19), 195112.

https://doi.org/10.1021/acs.inorgchem.2c03208
Inorg. Chem. 2022, 61, 20206−20210